

A Systematic Evaluation of GPT-4V's Multimodal Capability for Medical Image Analysis

Yunyi Liu^{a,*}, Yingshu Li^{a,*}, Zhanyu Wang^{a,d,*}, Xinyu Liang^e, Lei Wang^b, Lingqiao Liu^c, Leyang Cui^d, Zhaopeng Tu^d, Longyue Wang^{d,**}, Luping Zhou^{a,**}

^aElectrical and Computer Engineering, The University of Sydney, NSW, 2006, Australia

^bSchool of Computing and Information Technology, The University of Wollongong, NSW, 2522, Australia

^cSchool of Computer and Mathematical Sciences, The University of Adelaide, Adelaide, 5005, Australia

^dTencent AI Lab, Tencent, Shenzhen, 518000, China

^eFirst Clinical Medical College, Guangzhou University of Chinese Medicine, Guangzhou, 510405, China

ARTICLE INFO

Keywords:

GPT-4V
Medical Image
Radiology Report Generation
Medical Visual Question Answering
Medical Visual Grounding
Large Language Model Evaluation

ABSTRACT

This work conducts an evaluation of GPT-4V's multimodal capability for medical image analysis, with a focus on three representative tasks of radiology report generation, medical visual question answering, and medical visual grounding. For the evaluation, a set of prompts is designed for each task to induce the corresponding capability of GPT-4V to produce sufficiently good outputs. Three evaluation ways including quantitative analysis, human evaluation, and case study are employed to achieve an in-depth and extensive evaluation. Our evaluation shows that GPT-4V excels in understanding medical images and is able to generate high-quality radiology reports and effectively answer questions about medical images. Meanwhile, it is found that its performance for medical visual grounding needs to be substantially improved. In addition, we observe the discrepancy between the evaluation outcome from quantitative analysis and that from human evaluation. This discrepancy suggests the limitations of conventional metrics in assessing the performance of large language models like GPT-4V and the necessity of developing new metrics for automatic quantitative analysis.

© 2024 Elsevier B. V. All rights reserved.

1. Introduction

Large language models (LLMs) have recently demonstrated remarkable ability across various domains and tasks (Touvron et al., 2023; OpenAI, 2023; Anil et al., 2023). The ongoing pursuit of enhancing LLMs' capability for visual comprehension has further spurred the emergence of large multimodal models (LMMs) (Ye et al., 2023; Li et al., 2023b; Awadalla et al., 2023). Among them, GPT-4V incorporates visual understanding capability by learning from an extensive corpus of multimodal data and demonstrates great potential on multimodal data comprehension. It is a state-of-the-art model known for its proficiency in image analysis and text generation. To have a precise understanding of GPT-4V's potential, research has been newly conducted to investigate its capability for generic images (Wu et al., 2023b). For example, Yang et al. (2023b) conducted a case study to assess GPT-4V's performance in general-purpose scenarios, revealing its robust visual comprehension ability.

LLMs could have enormous applications to medicine and healthcare (Wang et al., 2023b; Singhal et al., 2023). The availability of vision module in GPT-4V opens up an opportunity for an in-depth examination of its potential in this regard. Some papers have started examining its performance on medical images (Wu et al., 2023a). However, they are primarily based on case studies.

In this work, we move beyond case studies and delve deeper into the capability of GPT-4V for multimodal tasks in medical image analysis. Our evaluations focus on three representative tasks in this regard, including radiology report generation, medical visual question answering, and medical visual grounding. This enables us to assess GPT-4V's ability in understanding and interacting between visual and textual modalities from various perspectives. Our evaluation takes a multifaceted approach consisting of quantitative analysis, human evaluations, and case studies. Quantitative analysis calculates conventional performance-related metrics and compares GPT-4V with other relevant models by following the protocols in the literature. Human evaluation is used to obtain a more precise assessment of the quality of text output of GPT-4V in the tasks of radiology report generation and medical visual question answering. This is particularly meaningful when considering that conventional

*Equal Contribution

**Corresponding author

e-mail: vinnylywang@tencent.com (Longyue Wang),
luping.zhou@sydney.edu.au (Luping Zhou)

metrics are not able to provide a direct and whole assessment. Case study is utilised to facilitate an intuitive understanding and assessment of the output. Altogether, the three evaluation methods offer an extensive view of the performance of GPT-4V.

Various prompt settings are explored in the evaluation of GPT-4V. Zero-shot prompts and few-shot prompts are tested for the task of radiology report generation based on whether a set of example reference reports is provided. For medical visual question answering, several examples are provided as prompts to guide GPT-4V to respond in a way that better aligns with the form of ground truth. For medical visual grounding, the prompt is mainly used to inform GPT-4V of the specific requirement of the output, particularly on creating the bounding boxes for visual grounding. Evaluation with the above prompt settings allows the capability of GPT-4V to be properly activated and its performance concerning prompt to be assessed.

The results of our evaluations are summarised as follows.

- GPT-4V demonstrates promising performance in generating radiology reports for medical images. Assessed by either language fluency related metrics or clinical efficacy related ones, its performance is competitive with that of the models specially developed for this task. In addition, compared with the conventional metrics used in quantitative analysis, the human evaluation suggests an even higher level of accuracy, relevancy, and richness of the radiology reports generated by GPT-4V.
- GPT-4V shows its ability in generating detailed answers for the task of medical visual question answering. Meanwhile, when compared with the relevant state-of-the-art methods, it only achieves modest performance when assessed by the conventional metrics. This is attributed to the low correlation between questions and the generated answers, the great diversity of the answers generated by GPT-4V, and the fixed format of the ground-truth answers in the benchmark dataset. Meanwhile, human evaluation suggests that GPT-4V’s answers are more accurate than what is indicated by the conventional metrics.
- The result of the medical visual grounding task highlights a significant room for improvement. GPT-4V struggles with accurately locating and identifying specific elements within medical images. This is consistent with the weakness revealed by existing evaluation on the tasks related to generic images. This finding points out a potential direction to further enhance GPT-4V’s performance.
- In addition to utilising conventional metrics, our evaluation also involves professional medical practitioners conducting human evaluation, adding a layer of expert review to our assessment. Their discrepancy reveals the limitations of conventional performance-related metrics in accurately assessing the performance of GPT-4V, highlighting the urgency of developing more proper ways of evaluation for LLMs.

The remainder of the paper is organized as follows. Section 2 is the related work for GPT-4V. Section 3 introduces our Evalua-

tion, which contains evaluation tasks, evaluation method, evaluation datasets and evaluation results. Section 4 describes our summary and discussion. We conclude the paper and discuss the limitation in Section 5.

2. GPT-4V (OpenAI, 2023)

GPT-4V, or GPT-4 with Vision, stands as an advanced multimodal system developed by OpenAI, integrating image inputs into LLMs. This groundbreaking fusion represents a notable frontier in AI research, enabling innovative interfaces and the solution of new tasks for unique user experiences. The system is built upon the GPT-4 model and has been trained on an extensive dataset comprising text and image data from the internet and licensed sources. GPT-4V showcases what can and cannot be done with text and image processing, highlighting new strengths that come from combining these two types of data. This includes advanced intelligence and the ability to reason across a broad range of topics.

Several recent publications have explored the multimodal capacities of GPT-4V. Early evaluations, as presented in (Wu et al., 2023b), offered insights into GPT-4V’s abilities and limitations. (Li et al., 2023d) focused on Visual Question Answering (VQA) tasks, while (Shi et al., 2023) explored GPT-4V’s Optical Character Recognition (OCR) capabilities. Some research works, like (Wu et al., 2023a), specifically investigated medical image tasks, albeit with a more case-study-oriented approach lacking in-depth exploration. In contrast, our paper aims to provide a deeper study of GPT-4V’s multimodal capabilities in medical imaging contexts.

3. Evaluation

The upcoming paragraphs provide a detailed introduction to four key components of our evaluation process.

Evaluation Tasks describes the specific tasks that we set up for the evaluation.

Evaluation Method outlines how we design the prompts and describes the methodology used to assess the models. This includes the criteria for evaluation, the metrics such as accuracy, precision, recall, F1 score, BLEU, CIDEr, ROUGE, METEOR, accuracy, and mIoU, and any specific protocols or procedures that we followed during the evaluation process.

Evaluation Datasets provides details about the datasets involved in the evaluation. Important aspects like the source, the sizes, and the characteristics of the datasets, as well as their relevance to the evaluation tasks, are discussed.

Evaluation Results presents the results of the evaluation. It includes a summary of the findings, comparisons with benchmarks or previous models (if applicable), and insights or interpretations of the results. It is partitioned into three parts: the quantitative, human evaluation, and case study results.

3.1. Evaluation Tasks

In the following, we introduce the three evaluation tasks shown in Figure 1, including radiology report generation (R2Gen), medical Visual Question Answering (VQA), and medical visual grounding (VG).

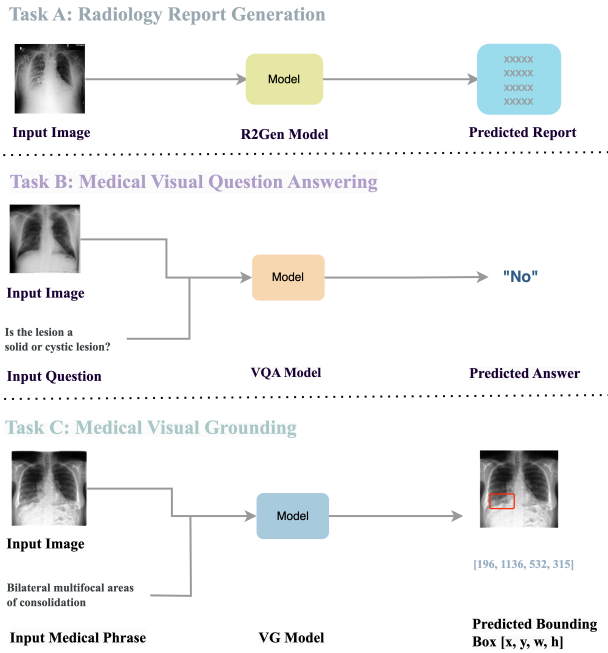


Fig. 1. Three multimodal medical imaging tasks we employ to evaluate GPT-4V’s performance.

3.1.1. Radiology Report Generation

Radiology report generation (R2Gen) is a very important application of medical images, akin to the task of image captioning (Vinyals et al., 2015; Xu et al., 2015; Pan et al., 2020). R2Gen poses unique challenges, given the inherent complexity of medical reports, their length, and the difficulty in discerning fine-grained abnormalities from medical images, particularly in datasets biased towards normal samples (referred to as data bias problem). Current research can be grouped into two primary research directions. The first direction concentrates on enhancing the model’s architecture to facilitate improved extraction of visual features and the generation of high-quality medical reports. For example, Li et al. (2018) used a hierarchical architecture to generate reports with normality and abnormality respectively. Building on the Transformer’s success (Vaswani et al., 2017), Chen et al. (2020) introduced a Transformer-based model, enhancing it with relational memory and memory-driven conditional layer normalization to enhance image feature representation and capture crucial report patterns (Chen et al., 2020). The second research direction addresses the data bias problem by incorporating external knowledge information. For example, some works constructed predefined medical knowledge graphs to augment the model’s ability to capture valuable clinical information (Zhang et al., 2020; Liu et al., 2021a; Li et al., 2023c; Huang et al., 2023b). Furthermore, very recently, there has been a surge in radiology report generation methods leveraging Large Language Models (LLMs). These approaches harness the capabilities of LLM to generate long-text content and utilise abundant knowledge sources to enhance the quality of radiology reports. For example, Wang et al. (2023b) employed LLaMA2 (Touvron et al., 2023) to elevate the quality of the generated reports, ensuring effective image-text alignment through a visual mapper.

3.1.2. Visual Question Answering

The Visual Question Answering (VQA) task (Jiang et al., 2020; Wu et al., 2019) involves processing the input image-question pairs to generate appropriate answers. Currently, there are two predominant approaches for implementing VQA tasks: classification-based (Nguyen et al., 2019; Finn et al., 2017; Es-lami et al., 2021), and generation-based (Ambati and Dudyala, 2018; Khare et al., 2021). By nature, VQA should be based on generation. The ongoing shift from a classification-centric paradigm to a generation-oriented approach represents a prevailing trend in the VQA field. Based on the characteristics of the VQA task, a proficient text generation model is essential. Consequently, the current surge in LLMs presents a significant opportunity for substantial improvements in the VQA task. Numerous endeavors incorporating LLMs into VQA tasks are already underway, whether for generating VQA datasets (Pellegrini et al., 2023) or utilising LLMs to enhance the performance of VQA systems (Li et al., 2023a). The evident improvements that LLMs bring to VQA lead us to believe that they are well-suited for this task. Consequently, evaluating the VQA task is a crucial aspect of GPT-4V’s evaluation.

3.1.3. Visual Grounding

In the visual grounding (VG) (Kamath et al., 2021) task, the input typically comprises a medical image accompanied by a descriptive statement about the image, often pertaining a specific medical sign or symptom. The task’s output is the coordinates of a bounding box that visually marks the area described in the statement, such as encapsulating a particular medical sign. Most visual grounding research focuses on general images, with only a few studies targeting medical images, likely due to the scarcity of corresponding medical datasets. However, the recently introduced MS-CXR dataset has opened up new possibilities in medical visual grounding, leading to emerging publications (Huang et al., 2023a; Sun et al., 2023a,b) based on this dataset. Despite growing recognition, there remains untapped potential, presenting a significant opportunity for future research in medical visual grounding. Unlike the previous two tasks, the output for visual grounding is not a conventional text paragraph but a set of coordinates. Recent studies have successfully integrated LLMs (Peng et al., 2023; Zhao et al., 2023) to directly produce these coordinates as outputs, showing promising results. Recognizing this potential, we hypothesize that GPT-4V should also possess visual grounding capabilities. Consequently, we include this task in our evaluations to assess GPT-4V’s performance in this specific area.

3.2. Evaluation Method/Process

3.2.1. Radiology Report Generation

To better activate the capabilities of GPT-4V, we explore various prompt design strategies, including the **zero-shot** and **few-shot** approaches.

Zero-shot Prompt: In zero-shot scenario, we provide a prompt without reference reports, allowing GPT-4V to autonomously generate reports without external guidance.

GPT-4V is tasked with generating both the “impression” and “findings” sections and compared with the ground truth report.

Few-shot Prompts: In-context few-shot learning represents a crucial methodology for enhancing the capabilities of LLMs (Tsimpoukelli et al., 2021; Wei et al., 2022a; Dai et al., 2022). It enables the model to acquire the expected output format by providing a set of examples. In contrast to fine-tuning, this method empowers the model to generate desired results without any parameter updating at inference time. In our investigation, we experiment with a few prompt strategies designed for GPT-4V. Specifically, we explore diverse compositions within the few-shot prompts:

- Exclusively using normal examples (**Few-shot normal-example prompt**),
- Exclusively using abnormal examples (**Few-shot abnormal-example prompt**), and
- Combining one normal and one abnormal example (**Few-shot mixed-example prompt**).

R2Gen prompt

Zero-shot prompt
You are a professional radiologist. I will provide you with some chest X-ray images. Please generate a radiology report based on the provided image. You should only generate reports and no other unnecessary information.

Few-shot normal examples prompt
You are a professional radiologist. I will provide you with some chest X-ray images. Please generate a radiology report based on the provided image. You should only generate reports and no other unnecessary information. The format of the output report should be similar to the example:
Examples:

Normal Example Report 1
Normal Example Report 2

Few-shot abnormal examples prompt
You are a professional radiologist. I will provide you with some chest X-ray images. Please generate a radiology report based on the provided image. You should only generate reports and no other unnecessary information. The format of the output report should be similar to the example:
Examples:

Abnormal Example Report 1
Abnormal Example Report 2

Few-shot mixed examples prompt
You are a professional radiologist. I will provide you with some chest X-ray images. Please generate a radiology report based on the provided image. You should only generate reports and no other unnecessary information. The format of the output report should be similar to the example:
Examples:

Abnormal Example Report 1
Normal Example Report 1

Fig. 2. R2Gen Prompt Examples. Three types of prompt settings are tested, including one zero-shot prompt and three few-shot prompts.

Our evaluation reveals that the inclusion of both normal and abnormal example reports consistently results in higher-quality report generation. More discussions about this finding are provided in our case study. Also, details regarding our selected example reports are given in Appendix A.1.2. Subsequently, we employ the **few-shot mixed-example prompt** to evaluate GPT-4V on the MIMIC-CXR benchmark (Johnson et al., 2019). Our primary focus lies on the **zero-shot** and **few-shot** scenarios, deliberately avoiding complex techniques such as chain-of-thought (Wei et al., 2022b) or ensembling strategies (Wang et al., 2022a) to manage the complexity of our efforts.

Evaluation Metrics: In our evaluation of the generated

reports, we calculate a range of metrics including BLEU, ROUGE, METEOR, and CIDEr. These metrics, widely recognized in the field of natural language processing (NLP), offer diverse perspectives on the quality of the generated text. BLEU measures the similarity of the generated text to a set of reference texts, focusing on the precision of word choices. ROUGE assesses the recall aspect, evaluating how much of the reference content is captured in the generated text. METEOR considers both precision and recall, accounting for synonymy and paraphrasing. CIDEr, originally developed for image captioning, evaluates the similarity of the generated text to multiple reference texts, emphasizing the consensus among them. Following the computation of these scores, we conduct human evaluations to ascertain the consistency between these computational assessments and human judgment. The human evaluation involves reviewers analysing the quality of the generated reports in terms of relevance, accuracy, coherence, and overall appropriateness. This combined approach of using both NLP metrics and human judgment is crucial for a more accurate evaluation. While metrics like BLEU, ROUGE, METEOR, and CIDEr offer quantitative insights into specific aspects of text quality, human evaluation provides a qualitative assessment, capturing subtleties and nuances that NLP metrics may overlook. By comparing the results from both evaluation methods, we validate the effectiveness of the generated reports from multiple perspectives, ensuring a comprehensive and reliable assessment of their quality. This process helps in determining whether the generated reports are not only linguistically correct but also contextually and semantically appropriate, aligning with human understanding and expectations.

3.2.2. Medical Visual Question Answering

For medical VQA, we employ the “few-shot prompt” strategy to address a significant limitation associated with the existing VQA datasets, namely the limited range of their predetermined answer set. To enhance the alignment of the answers generated by GPT-4V with the dataset, our strategy involves introducing GPT-4V to the concept of categorizing VQA questions based on the expected answer types. This approach enables the model to differentiate between close-end questions typically requiring short and concise answers (e.g., “yes” or “no”), and open-end questions demanding more detailed responses. By training GPT-4V with this categorization approach, we enhance GPT-4V’s ability to adapt the length of its responses appropriately. For close-end questions, it learns to provide brief answers, while for open-end ones, it comprehends the need for more elaborate responses. This nuanced response mechanism significantly improves the relevance and accuracy of GPT-4V’s answers, thereby increasing the effectiveness of our evaluations.

VQA Prompt: Our VQA prompt follows the template in Figure 3. We provide seven examples to guide the model in generating responses consistent with the dataset’s format. Without these examples, GPT-4V tends to produce more unconstrained answer text, complicating the task of comparing the predicted answers with the ground truth.

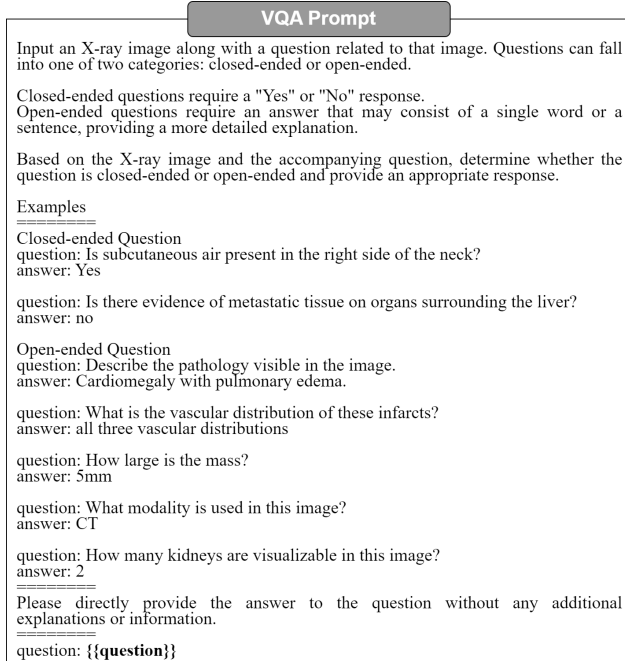


Fig. 3. VQA Prompt Example. The content between the double braces is replaced with specific questions.

Evaluation Metrics: To analyse GPT-4V’s performance in medical VQA, we employ different evaluation metrics for close-end and open-questions, respectively. For close-end questions, we calculate the model’s prediction accuracy and compare its performance with that of the state-of-the-art (SOTA) VQA methods which are mainly classification-based approaches. This comparison is crucial to understanding how GPT-4V ranks in the current landscape of VQA technologies, especially those tailored for medical applications. For open-end questions, we calculate BLEU scores (specifically, BLEU-4), a widely used metric in NLP to assess the quality of machine-generated text. This choice is based on the nature of open-end questions which typically require more detailed and varied responses than close-end questions. Unlike close-end questions with straightforward single-word answers, open-end questions permit a range of possible correct answers, each potentially phrased differently. After calculating the BLEU scores for open-end questions, we proceed to human evaluation to assess the consistency between the BLEU scores and human judgment. This step is crucial for a more effective evaluation of the accuracy of the generated answers. Human evaluation involves a trained radiologist reviewing and rating the quality of the model-generated answers. This method is particularly valuable as BLEU scores, while offering a quantitative measure of text similarity, might not fully capture the nuances of meaning, relevance, and context that human evaluators can discern. By comparing the outcomes of the BLEU score analysis with human assessments, we gain a more holistic understanding of the GPT-4V’s performance. This dual approach of combining BLEU scores with human evaluation allows us to cross-verify the effectiveness of the model’s answers.

3.2.3. Medical Visual Grounding:

For the Medical Visual Grounding (VG) task, we employ a straightforward prompt without incorporating examples. We opt for this approach to prevent potential restrictions on GPT-4V’s response to only those scenarios covered in the examples, thus preserving its ability to generalize. Our goal is to avoid steering the model towards producing results solely based on the provided examples. In our prompt design, we focus solely on informing GPT-4V about the required output format, i.e., the coordinates of the bounding box. This approach guides the model in understanding our specific requirements, particularly in generating bounding boxes for visual grounding tasks.

Visual Grounding Prompt: We design a specific type of prompt that significantly improves the model’s understanding and its ability to accurately generate bounding boxes. The prompt is illustrated in Figure 4.

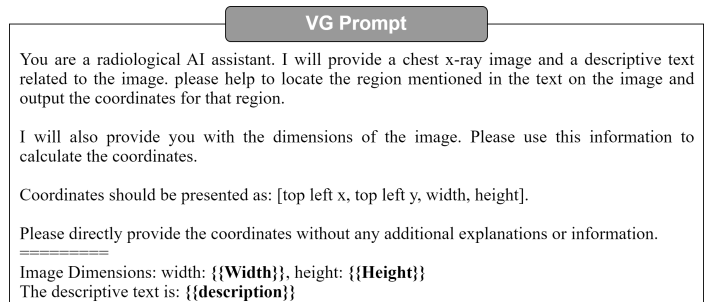


Fig. 4. VG Prompt Example. The content between double braces is replaced with specific image width, height, and description text related to the image.

Evaluation Metrics: We evaluate by calculating the mean Intersection over Union (mIoU) across all samples in the benchmark dataset. The mIoU metric is a standard measure used in the field to assess the accuracy of object localization and segmentation in images. By computing the mIoU, we could gauge how precisely the GPT-4V identifies and outlines relevant areas in the images compared to the ground truth. After calculating the mIoU, we conduct a comparative analysis with the SOTA VG methods. This comparison allows us to benchmark GPT-4V’s performance against the currently leading methods in the field. By comparing the mIoU results of GPT-4V with those of the SOTA methods, we could gain a clear understanding of the strengths and weaknesses of GPT-4V in the context of the broader research landscape.

3.3. Evaluation Datasets

Radiology Report Generation Dataset: MIMIC-CXR (Johnson et al., 2019), the largest publicly available dataset in this domain, includes both chest radiographs and unstructured textual reports. This dataset comprises a total of 377,110 chest X-ray images and 227,835 corresponding reports, obtained from 64,588 patients who underwent examinations at the Beth Israel Deaconess Medical Center between 2011 and 2016. To facilitate fair and consistent comparisons, we follow the official

partitioning provided by MIMIC-CXR, resulting in a test set containing 3,858 samples. For human evaluation, 100 report pairs comprising both the ground truth and their corresponding reports generated by GPT-4V are randomly selected from the MIMIC-CXR dataset and rated by a trained radiologist.

VQA Dataset: VQA-RAD (Lau et al., 2018) is one of the most widely utilised radiology datasets. It comprises 315 images along with 3515 question-answer pairs, ensuring that each image corresponds to at least one question-answer pair. The questions encompass 11 distinct categories, including “anomalies”, “properties”, “color”, “number”, “morphology”, “organ type”, “other”, and “section”. A noteworthy 58% of these questions are designed as close-end queries, while the remainder takes the form of open-end inquiries. These images predominantly feature the head, chest, and abdomen regions of the human body. The dataset is officially partitioned into a training subset of 3064 question-answer pairs and a test subset of 451 question-answer pairs for evaluation. For human evaluation, 100 open-end question-answer pairs are randomly selected from the VQA-RAD dataset and marked by a trained radiologist.

Visual Grounding Dataset: MS-CXR (Boecking et al., 2022) dataset is a valuable resource for biomedical vision-language processing, featuring 1162 image-sentence pairs with bounding boxes and corresponding phrases. It was meticulously annotated by board-certified radiologists, covering eight cardiopulmonary radiological findings, each having an approximately equal number of pairs. This dataset offers both reviewed and edited bounding boxes/phrases and manually created bounding box labels from scratch. What sets MS-CXR apart is its focus on complex semantic modeling and real-world language understanding, challenging models with joint image-text reasoning and tasks like parsing domain-specific location references, complex negations, and variations in reporting style. It serves as a benchmark for phrase grounding and has been instrumental in demonstrating the effectiveness of principled textual semantic modeling for enhancing self-supervised vision-language processing.

3.4. Evaluation Result

3.4.1. Quantitative Results

Radiology Report Generation

Comparison with SOTA Methods: Table 2 presents a performance comparison between the GPT-4V model and SOTA methods using the MIMIC-CXR dataset (Johnson et al., 2019). The comparison methods encompass standard image captioning techniques, including Show-Tell (Vinyals et al., 2015), Att2in (Xu et al., 2015), AdaAtt (Lu et al., 2017), Transformer (Vaswani et al., 2017), and M2Transformer (Cornia et al., 2020). Additionally, we compare with the radiology report generation methods, specifically R2Gen (Chen et al., 2020), R2GenCMN (Chen et al., 2021), MSAT (Wang et al., 2022b), and METransformer (Wang et al., 2023a). As aforementioned, we employ few-shot mixed-example prompts to help GPT-4V generate medical reports. From Table 2, it is

clear that radiology report generation models such as METransformer, MSAT, and R2Gen exhibit top-tier performance. Nevertheless, GPT-4V’s capability to generate medical reports is impressive, considering it is designed as a general-purpose model. Leveraging the advantages of an extensive dataset for pretraining, GPT-4V performs well in several metrics, including BLEU (Papineni et al., 2002), ROUGE (Lin, 2004), and METEOR (Banerjee and Lavie, 2005). However, when compared to models specifically trained on MIMIC-CXR, GPT-4V exhibits a performance gap, particularly evident in CIDEr (Vedantam et al., 2015). This discrepancy arises because the CIDEr metric differently scores words based on their occurrence frequencies, potentially affecting GPT-4V’s performance when it fails to generate certain MIMIC-CXR-specific words, yielding relatively lower scores. Our evaluation reveals that GPT-4V possesses the capacity to generate information not present in the ground truth but visually evident in the image. This phenomenon contributes to GPT-4V’s relatively lower performance on metrics such as BLEU which primarily assesses word-match rates. One example is shown in Figure 5.

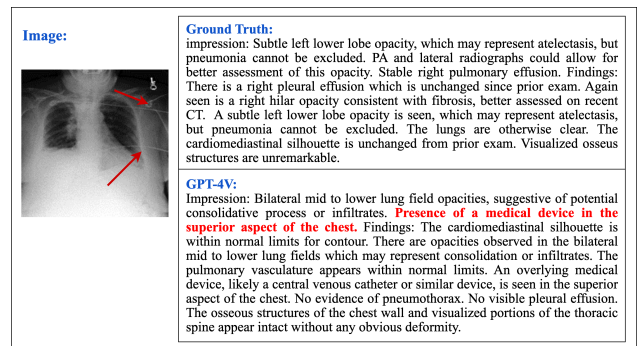


Fig. 5. An illustration of GPT-4V’s capability in generating medical reports using our designed few-shot mixed-example prompt. The ground truth does not mention a medical device but one is visibly present in the image, marked by red arrows. GPT-4V demonstrates the ability to recognize and describe the medical device in the generated report.

Clinical Efficacy on MIMIC-CXR Dataset: We assess the clinical efficacy of the GPT-4V model on the MIMIC-CXR dataset, which achieves a precision of 0.353, recall of 0.365, and F1 score of 0.330 in Table 2. Numerically, these results are not too bad compared to the two high-performing models METransformer (Wang et al., 2023a) and R2GenGPT (Wang et al., 2023b). GPT-4V demonstrates competitive clinical efficacy. Notably, the gap between GPT-4V and other models in terms of clinical efficacy is relatively smaller than that observed in traditional NLP metrics which primarily measure lexical overlap with ground truth reports. This suggests that, objectively, GPT-4V exhibits an impressive capability in radiology report generation, emphasizing its potential clinical accuracy and practicality.

Medical Visual Question Answering

Table 3 shows a performance comparison between the GPT-4V model and SOTA VQA methods using the VQA-RAD dataset. The compared methods include StAn (He et al., 2020), BiAn (He et al., 2020), MAML (Finn et al., 2017),

Table 1. Comparison on the MIMIC-CXR dataset.

Methods	BLEU-1	BLEU-2	BLEU-3	BLEU-4	ROUGE	METEOR	CIDEr
Show-Tell (Vinyals et al., 2015)	0.308	0.190	0.125	0.088	0.256	0.122	0.096
Att2in (Xu et al., 2015)	0.314	0.198	0.133	0.095	0.264	0.122	0.106
AdaAtt (Lu et al., 2017)	0.314	0.198	0.132	0.094	0.267	0.128	0.131
Transformer (Vaswani et al., 2017)	0.316	0.199	0.140	0.092	0.267	0.129	0.134
M2Transformer (Cornia et al., 2020)	0.332	0.210	0.142	0.101	0.264	0.134	0.142
R2Gen (Chen et al., 2020)	0.353	0.218	0.145	0.103	0.277	0.142	-
R2GenCMN (Chen et al., 2021)	0.353	0.218	0.148	0.106	0.278	0.142	-
PPKED (Liu et al., 2021b)	0.360	0.224	0.149	0.106	0.284	0.149	0.237
GSK (Yang et al., 2021)	0.363	0.228	0.156	0.115	0.284	-	0.203
MSAT (Wang et al., 2022b)	0.373	0.235	0.162	0.120	0.282	0.143	0.299
METransformer (Wang et al., 2023a)	0.386	0.250	0.169	0.124	0.291	0.152	0.362
GPT-4V (OpenAI, 2023)	0.338	0.190	0.109	0.061	0.240	0.125	0.033

Table 2. Evaluation of Clinical Efficacy on MIMIC-CXR dataset.

Models	Precision	Recall	F1
METransformer (Wang et al., 2023a)	0.364	0.309	0.334
R2GenGPT (Wang et al., 2023b)	0.392	0.387	0.389
GPT-4V	0.353	0.365	0.330

Table 3. Results on VQA-RAD benchmark

Reference Methods	Fusion Method	Accuracy (%) (Close-end)	BLEU-4 (Open-end)
StAn (He et al., 2020)	SAN	57.2	-
BiAn (He et al., 2020)	BAN	67.9	-
MAML (Finn et al., 2017)	SAN	69.7	-
	BAN	72.4	-
MEVF (Nguyen et al., 2019)	SAN	74.1	-
	BAN	75.1	-
MMQ (Do et al., 2021)	SAN	75.7	-
	BAN	75.8	-
PubMedCLIP (Eslami et al., 2021)	-	80	-
MMBERT (Khare et al., 2021)	-	77.9	-
Q2ATransformer (Liu et al., 2023)	-	81.2	-
GPT-4V (OpenAI, 2023)	-	61.40	0.1155

MEVF (Nguyen et al., 2019), MMQ (Do et al., 2021), Pub-MedCLIP (Eslami et al., 2021), MMBERT (Khare et al., 2021), and the Q2ATransformer (Liu et al., 2023). Recall that we report accuracies for close-end questions and BLEU scores for open-end questions. From Table 3, it can be seen that GPT-4V achieves an accuracy of 61.4% for the close-end questions, notably lower than other published results. In our experiment, we meticulously define open-end and close-end questions for GPT-4V in our prompt design, intending to guide its response generation effectively. Despite this, we observe that GPT-4V sometimes produces relatively long answers even for close-end questions that typically require brief single-word responses, such as “yes” or “no”. This deviation from the expected answer format leads to a lower accuracy score for these instances. Additionally, GPT-4V’s BLEU score for open-end questions is also modest at 0.116. This can be attributed to GPT-4V’s robust text generation capacity, leading to a greater diversity in its outputs. For example, GPT-4V can represent the same object in multiple ways leading to varied responses. This diversity suggests that traditional evaluation metrics like BLEU, which are based primarily on the overlap of words and lack of a deep understanding of textual meaning, are insufficient to assess the quality of GPT-4V’s varied answers. Given this limitation, we complement our evaluation with human assessments in Section 3.4.2 to provide a more appropriate and comprehensive evaluation. Human evaluation can capture subtleties and interpretations that purely text-based metrics like BLEU may overlook, especially when GPT-4V’s responses exhibit diversity and nuance beyond the scope of traditional metrics.

Medical Visual Grounding

Table 4 reports a comparative performance of GPT-4V against various SOTA visual grounding methods using the MS-CXR dataset. We compare GPT-4V with a range of advanced methods in the field: BioViL (Boecking et al., 2022), BioViL-T (Bannur et al., 2023), RefTR (Li and Sigal, 2021), VGTR (Du et al., 2022), SeqTR (Zhu et al., 2022), TransVG (Deng et al., 2021), and MedRPG (Chen et al., 2023). Each of these models represents a significant approach or innovation in medical image analysis, making them suitable benchmarks for evaluating GPT-4V’s performance. By using the mIoU metric, we can quantitatively assess how well GPT-4V and other models perform in terms of accurately identifying and delineating relevant patterns within the medical images of the MS-CXR dataset. GPT-4V’s performance on the MS-CXR dataset yields an mIoU of 0.083, significantly lower than all published benchmarks. While GPT-4V demonstrates a level of comprehension in visual grounding, it struggles to accurately identify medical organs and pathological signs, leading to imprecise bounding box predictions. It should be noted that the recent SoM (Yang et al.,

2023a) model has shown substantial improvements in this area by segmenting and labeling images before grounding, enhancing performance on generic images. However, its effectiveness on medical images demanding finer details remains untested. Further research is necessary to assess its applicability to medical imaging.

Table 4. mIoU(%) results on MS-CXR benchmark.

Methods	mIoU(%)
BioViL (Boecking et al., 2022)	22.9
BioViL-T (Bannur et al., 2023)	24.3
RefTR (Li and Sigal, 2021)	50.11
VGTR (Du et al., 2022)	53.58
SeqTR (Zhu et al., 2022)	56.63
TransVG (Deng et al., 2021)	58.91
MedRPG (Chen et al., 2023)	59.37
GPT-4V (OpenAI, 2023)	8.33

3.4.2. Human Evaluation Results

This section details our approach to evaluating and analysing human assessments of radiology reports and VQA tasks. Specifically, we choose not to include human evaluation for the visual grounding task. The reason is that the output of visual grounding is typically a simple bounding box, rather than text. The quality of these bounding boxes can be straightforwardly assessed through visualization, making human evaluation less critical for this aspect. However, when it comes to the evaluation of text generation, visual inspection of the words alone is insufficient for determining quality. The key aspect of evaluating the text produced by a large-scale model like GPT-4V lies in understanding the semantic meaning of the generated content. Text quality encompasses more than just the correct words. Therefore, we incorporate human evaluation as a crucial part of our assessment process for text generation. Human evaluators can provide insights into how well the model captures the intended meaning, context, and subtleties that traditional metrics may overlook. This approach allows for a more nuanced and comprehensive evaluation of the quality of text generated by GPT-4V.

Radiology Reports Human Evaluation

We conduct a random selection of 100 report pairs, including corresponding ground truth reports and the reports generated by GPT-4V. These pairs undergo grading by a trained radiologist, categorized into three levels: high, medium, and low, based on varying degrees of human-perceived consistency. Simultaneously, we calculate NLP scores for BLEU, ROUGE, METEOR, and CIDEr for these 100 report pairs, focusing on BLEU and CIDEr due to minimal variation in ROUGE and METEOR.

Visualization & Distribution Analysis: Figure 6 presents scatter graphs illustrating the relationship between the BLEU/CIDEr/F1 scores and human ratings, respectively. The x-axis represents BLEU/CIDEr/F1 scores, while the y-axis de-

picts corresponding human scores for the same samples. Notably, a significant number of GPT-4V-generated reports with low BLEU scores (< 0.20) receive “Medium” or “High” quality evaluations in human ratings, a trend also observed with CIDEr metrics. The human rating is better aligned with the F1 score reflecting clinical efficacy, e.g., there are fewer reports with low F1 scores (< 0.20) rated as ‘Medium’ or ‘High’ by the human evaluator.

To align NLP scores with human ratings, we scale them to the range of [0, 100] using the formula $\hat{s} = \frac{s - \text{lowest}}{\text{highest} - \text{lowest}} \times 100$, where s is the original score, and \hat{s} is the scaled score. We quantize these scores into three quality ranges: low [0 40), medium [40 70), and high [70 100]. The distributions of the 100 samples are shown in Fig 6, corresponding to BLEU, CIDEr, F1, human rating, respectively. Specifically, based on the human rating, there are 10 high-, 35 medium-, and 55 low-quality reports; based BLEU scores, there are 1 high-, 2 medium-, and 97 low-quality reports; based on CIDEr, there are 5 high-, 53 medium-, and 42 low-quality reports; and based on F1 score, there 3 high-, 29 medium-, and 68 low-quality reports. Our findings indicate that traditional evaluation methods tend to yield lower scores compared to radiologist assessments, suggesting that human evaluation assigns higher scores to the reports generated by GPT-4V, implying better report quality than indicated by traditional scores.

Correlation & Statistical Test: To further assess the correlation between the NLP scores and human ratings, we calculate Kendall’s τ coefficient (i.e., Kendall rank correlation coefficient), which measures the ordinal association between two quantities. Kendall’s τ is defined as follows:

$$\tau = \frac{\text{number of concordant pairs} - \text{number of discordant pairs}}{\text{total number of pairs} \times (\text{total number of pairs} - 1)/2}$$

Concordant pairs occur when both the human evaluator and the NLP metric agree on the ranking of two reports. Conversely, discordant pairs occur when there is a disagreement between the rankings by the human evaluator and the NLP metrics. The τ coefficient is within the range $-1 \leq \tau \leq 1$. If two random variables are independent, the expectation of τ is zero. In addition, a statistical test with the null hypothesis of $\tau = 0$ (no correlation) is conducted, and the p-value is reported. The p-value helps determine whether the observed agreement or disagreement in rankings between human ratings and NLP metrics is statistically significant or due to random variations.

As reported in Table 5, for the NLP scores BLEU, ROUGE, METEOR, and CIDEr, the Kendall’s τ coefficients are small values around zero, suggesting the human rating and these NLP metrics are potentially independent. This is further supported by their corresponding large p-values, all exceeding 0.1, indicating a failure to reject the null hypothesis. Thus, the correlations between human ratings and NLP metrics are not statistically significant. However, the F1 score has a small p-value of 0.002 and a moderate Kendall’s τ of 0.242, showing a statistically significant rank correlation with the human rating. In short, the statistic tests support our observations that i) the quality of GPT-4V’s generated reports could be much higher than what traditional evaluation methods indicate; and ii) GPT-4V’s

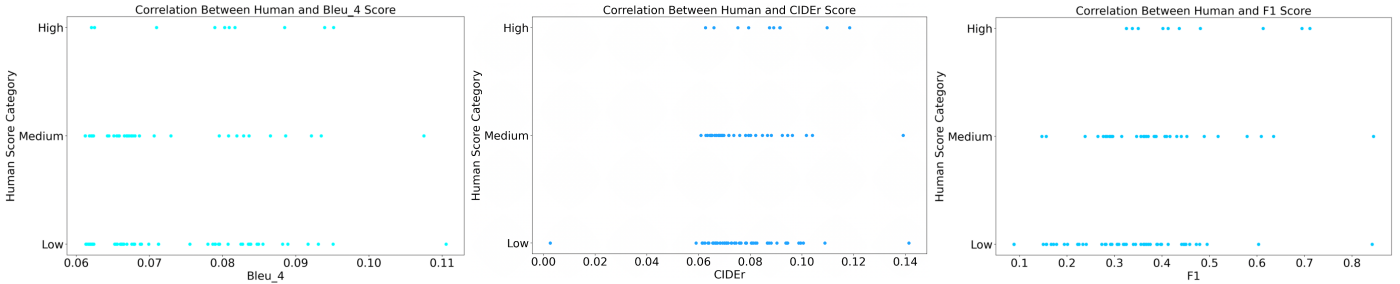


Fig. 6. Scatter graphs show the relationship between BLEU/CIDEr/F1 score and the human evaluation, respectively.

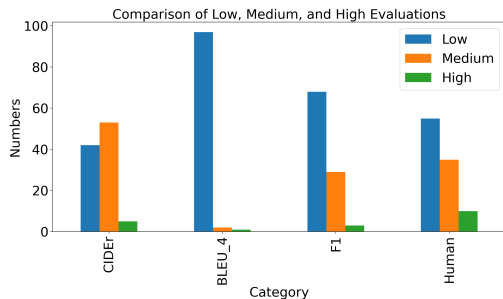


Fig. 7. Distributions of scores based on human evaluation, BLEU, CIDEr, and F1, respectively.

performance in clinical efficacy aligns with human evaluation, which are higher than NLP-based metrics. On the other hand, it should also be noted that human evaluation captures more than the clinical score of F1, as the latter is still limited in detecting the occurrence of clinically relevant keywords in the generated reports without comprehending the context.

An Example of Human Evaluation: To further bolster the credibility of our report generation results, we present an in-depth analysis conducted by a radiologist. This expert evaluation delves into the accuracy, relevance, and overall quality of the generated reports, providing valuable professional insights. The following example illustrates a notable disparity between BLEU scores and human evaluation. It juxtaposes a ground truth report with a report generated by GPT-4V, revealing that despite a low BLEU score, the report receives a high rating from a radiologist.

Ground Truth Report: “*Impression: Bilateral parenchymal opacities right greater than left compatible with pneumonia in the proper clinical setting. Findings : There bilateral regions of consolidation at the right lung and left mid to lower lung. Findings are most concerning for bilateral infection. Moderate enlargement of the cardiac silhouette is unchanged. Multiple vascular stents are also noted. No acute osseous abnormalities. splenic calcifications are again noted.*”

GPT-4V Predicted: “*Impression: Bilateral patchy opacities with potential for infiltrates or infectious etiology. Right-side mediastinal shift observed. Findings: The cardiomeastinal silhouette shows right-side deviation, which might be suggestive of volume loss or other pathology on the left side. Bilateral*

patchy opacities are noted which can represent infiltrates, raising concerns for potential infectious etiology, interstitial disease, or other inflammatory processes. The pulmonary vasculature appears within normal limits. There are no clear signs of pleural effusion or pneumothorax. The osseous structures of the thorax appear intact without evidence of acute fractures.”

Upon expert examination, the radiologist affirms that the predicted report accurately identifies key bilateral lung consolidation areas, describes the patchy morphology of the lesions, and provides insightful pathological inferences. The changes in the mediastinal position of the heart are also consistent with the original report. Although the direct determination of cardiac hypertrophy is not made, a positive prompt is acknowledged, aligning with chest X-ray reporting principles. Other negative diagnosis descriptions are basically consistent with the ground truth report. Consequently, the generated report receives a high score based on these professional evaluations.

	Bleu-4	ROUGE_L	METEOR	CIDEr	F1
P Value	0.688	0.430	0.462	0.503	0.002
Kendall’s Tau	0.032	0.063	0.059	0.053	0.242

Table 5. Evaluation of P Value and Kendall’s Tau

Visual Question Answering Human Evaluation

For this evaluation, we randomly select 100 open-end questions from VQA-RAD, together with ground truth and GPT-4V generated answers. A trained radiologist assesses the correctness of GPT-4V’s answers, identifying 57 answers as correct and 43 answers as incorrect. This contrasts sharply with the traditional accuracy metric used in the predominant classification-based VQA approaches, which detects only 9 correct answers, as shown in Figure 8. This disparity is rooted in the traditional classification-based VQA evaluation, which treats each predetermined answer as a class and calculates the classification accuracy. This evaluation lacks flexibility in handling the variability of answers produced by GPT-4V. Our human evaluation finds GPT-4V’s answers more accurate than traditional scores, highlighting the richness of content in GPT-4V’s responses not fully captured by conventional scoring methods. This underscores that the quality of GPT-4V’s answers is not inferior.

Moreover, delving into the answers generated by GPT-4V, the radiologist finds GPT-4V not only matches but surpasses the accuracy of the ground truth. This superiority is attributed to the detailed and precise nature of GPT-4V’s responses. Fig-

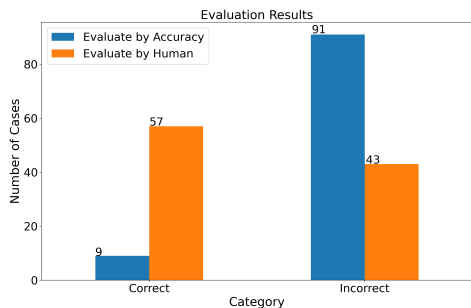


Fig. 8. Human evaluation of the correctness of the answers generated by GPT-4V on a subset of VQA-RAD, in contrast to the evaluation based on the classification accuracy of the same dataset.

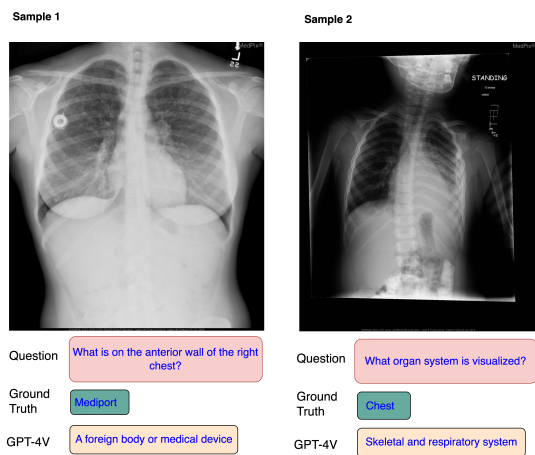


Fig. 9. Two examples showcase GPT-4V’s performance on open-end questions.

Figure 9 provides two VQA examples produced by GPT-4V. In the right example, given the question “what organ system is visualized”, the ground truth provided only mentions the chest, which is neither rigorous nor sufficient. In contrast, GPT-4V’s response includes the skeleton and respiratory system, demonstrating improved accuracy and completeness. Moreover, the answers generated by GPT-4V exhibit a higher level of generalization and comprehensiveness. As shown in the left example, GPT-4V describes “mediport” as “A foreign body or medical device”. Additionally, GPT-4V produces answers that are more professional and readable, presenting complete sentences with medical terminology and grammatical accuracy. These findings suggest that GPT-4V holds significant learning potential, inviting further exploration through additional research.

3.4.3. Case Study

In this part, we demonstrate GPT-4V’s performance by incorporating case studies across the three specific tasks, offering a more direct and intuitive view of its capabilities.

Radiology Report Generation Cases

In zero-shot scenarios, through a series of tests on multiple chest X-ray images, it is observed that GPT-4V consistently generates reports with a focus on specific anatomical organs.

This phenomenon can be observed in Figure 10. Notably, GPT-4V tends to present information in a specific sequence, covering the information on the lung, cardiomeastinal silhouette, bones, diaphragm, and soft tissues, in the majority of the generated reports. Examining the third case in Figure 10, GPT-

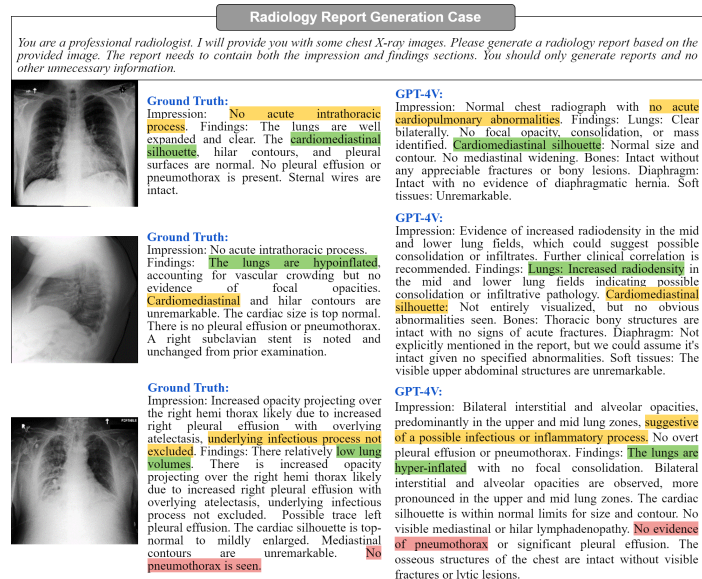


Fig. 10. R2Gen case using zero-shot prompt. GPT-4V can generate radiology reports without example reports and convey both normal and abnormal aspects. For better illustration, the key medical information in the reports is highlighted using different colours.

4V demonstrates its proficiency to identify both normal and abnormal aspects, e.g., “No pleural effusion or pneumothorax is present; Suggestive of a possible infectious or inflammatory process”. These instances underscore GPT-4V’s ability, even with zero-shot prompts, to generate relevant reports and identify anomalies.

In few-shot scenarios, our observation indicates that different prompts significantly influence the generated reports. GPT-4V’s inclination to generate normal or abnormal findings varies based on the provided example reports. Figure 11 illustrates the response to a normal chest X-ray image, utilising three distinct prompt settings to guide GPT-4V in generating corresponding reports. Interestingly, it is found that the report generated either from the normal-example prompt or the mixed-example prompt describes the image as normal, which is consistent with the ground truth. In contrast, the report from the abnormal-example prompt misidentifies anomalies in the image. Meanwhile, Figure 12 showcases an example of an abnormal chest X-ray image. It is observed that the report generated by the normal-example prompt misinterprets the lungs as normal. Our investigation emphasizes the substantial impact of the mixed-example prompt on GPT-4V’s accuracy in determining the normality or abnormality of an image.

Visual Question Answering Cases

We delve into specific cases of VQA illustrated in Figures 13, and 14. Figure 13 presents two examples of the close-end questions with a single-word answer of “yes” or “no”. Effectively

Radiology Report Generation Case

Text-Prompt:

You are a professional radiologist. I will provide you with some chest X-ray images. Please generate a radiology report based on the provided image. You should only generate reports and no other unnecessary information. The format of the output report should be similar to the example:

Examples:
=====

Example 1

Example 2

Image:



Ground Truth:

Impression: No acute intrathoracic process.
Findings: The lungs are well expanded and clear. The cardiomeastinal silhouette, hilar contours, and pleural surfaces are normal. No pleural effusion or pneumothorax is present. Sternal wires are intact.

Few-shot mixed examples prompt:

Impression: Normal cardiopulmonary findings with no acute abnormalities. Findings: Frontal view of the chest demonstrates clear lung fields without focal consolidations, masses, or opacities. The cardiomeastinal silhouette and pulmonary vasculature are within normal limits. Both hemidiaphragms are intact with no evidence of elevation. There is no visible pneumothorax, pleural effusion, or significant lymphadenopathy. The bony thoracic structures appear intact without any evident pathological changes.

Few-shot normal examples prompt:

Impression: No acute cardiopulmonary abnormalities noted. Findings: The lungs are clear without any evidence of consolidation, pleural effusion, or pneumothorax. The cardiomeastinal silhouette is within normal limits. There is no evidence of pulmonary nodules or masses. No significant bony abnormalities are noted in the imaged portions of the chest. The imaged upper abdomen appears unremarkable.

Few-shot abnormal examples prompt:

Impression: Increased opacity in the left lower lung zone, consistent with consolidation or infiltrate, which may suggest pneumonia. Mediastinal and cardiac contours are within normal limits. Findings: PA view of the chest demonstrates an increased opacity in the left lower lung zone, which may be secondary to consolidation or infiltrate. The lungs are otherwise well aerated. No evidence of pneumothorax or pleural effusion. The mediastinal and cardiac contours appear within normal limits. No visible pulmonary nodules or masses. No evidence of mediastinal widening or adenopathy. The bony thorax and soft tissues appear unremarkable.

Fig. 11. R2Gen normal case. Key medical information in the reports is highlighted using different colors. GPT-4V is more likely to generate reports containing abnormality descriptions when the prompt consists of only abnormal examples. The text in red corresponds to descriptions of abnormal conditions.

addressing such questions requires GPT-4V to accomplish two key tasks: firstly, discern that the question is close-end, and secondly, comprehend the attributes of a close-end question. This proficiency is crucial because, despite the simplicity of these questions, GPT-4V tends to generate more extended responses, which will be deemed incorrect when assessing the accuracy of answers to close-end questions. Thus, GPT-4V faces the challenge of identifying when a question demands a concise one-word answer and adjusting its response generation accordingly. Properly tailoring its output to match the question type is essential for GPT-4V’s accuracy in dealing with close-end questions.

Open-end questions demand more intricate responses beyond a simple “yes” or “no”, providing flexibility in generating answers. However, for the VQA task, the challenge lies in predefined answer pools, making it hard for GPT-4V to generate an exact sentence that matches these predefined answers. In Figure 14, we present two examples of open-end questions. The first example showcases a correct, succinct response from GPT-4V, consisting of just one word. This showcases GPT-4V’s effective handling of simple, direct open-end questions. The second example, however, depicts an incorrect answer by GPT-4V. The response provided by GPT-4V is a detailed explanation of the brain structures potentially affected by a lesion in the right frontal area, encompassing the prefrontal cortex, primary motor cortex, and possibly the premotor and precentral gyrus. This response appears more fitting for a theoretical question about brain anatomy, such as “What brain structures would be affected by a lesion in the right frontal area of the brain?” In this case, GPT-4V seems to have relied solely on medical knowledge without adequately considering the specific image in question. This suggests that GPT-4V might sometimes overlook the visual information in VQA tasks, especially when the question can be addressed through general medical knowledge.

Radiology Report Generation Case

Text-Prompt:

You are a professional radiologist. I will provide you with some chest X-ray images. Please generate a radiology report based on the provided image. You should only generate reports and no other unnecessary information. The format of the output report should be similar to the example:

Examples:
=====

Example 1

Example 2

Image:



Ground Truth:

Impression: Increased opacity projecting over the right hemi thorax likely due to increased right pleural effusion with overlying atelectasis, underlying infectious process not excluded. Findings: There relatively low lung volumes. There is increased opacity projecting over the right hemi thorax likely due to increased right pleural effusion with overlying atelectasis, underlying infectious process not excluded. Possible trace left pleural effusion. The cardiac silhouette is top-normal to mildly enlarged. Mediastinal contours are unremarkable. No pneumothorax is seen.

Few-shot mixed examples prompt:

Impression: Bilateral interstitial opacities, potentially indicating interstitial lung disease or atypical infection. Findings: Frontal view of the chest shows bilateral interstitial opacities, more prominent in the upper lobes. The cardiomeastinal silhouette is within normal limits. Pulmonary vasculature appears normal. Possible show pleural effusion. No evidence of pneumothorax. The diaphragms are at the appropriate levels, and bony thorax appears intact with no obvious fractures.

Few-shot normal examples prompt:

Impression: No acute cardiopulmonary abnormalities detected. Findings: The lungs are clear without evidence of focal consolidation, pleural effusion, or pneumothorax. The cardiomeastinal silhouette is within normal limits. No prominent hilar or mediastinal lymphadenopathy is seen. There is no evidence of pulmonary edema. The visualized bony structures appear intact without acute fractures or lesions. The imaged upper abdomen is unremarkable.

Few-shot abnormal examples prompt:

Impression: Bilateral patchy opacities observed, possibly indicative of a pneumonia or interstitial lung disease. Elevated right hemidiaphragm. Findings: The provided chest X-ray demonstrates bilateral patchy opacities predominantly involving the upper and mid lung zones. The right hemidiaphragm appears elevated compared to the left, suggesting possible diaphragmatic dysfunction or underlying right basal atelectasis. The heart size appears within normal limits. No overt pleural effusion is noted. The cardiomeastinal silhouette is unremarkable without any significant lymphadenopathy. The osseous structures are intact with no evident bony pathology.

Fig. 12. R2Gen abnormal case. Key medical information in the reports is highlighted using different colors. GPT-4V is more likely to generate normal reports when the prompt consists of only normal examples. The text in red corresponds to descriptions of normal conditions.

This insight underscores the challenge GPT-4V faces to generate responses for open-end VQA tasks.

Visual Question Answering Cases (Close-end Questions)

<p>Text-Prompt:</p> <p>Input an X-ray image along with a question..... (VQA Prompt)</p> <p>=====</p> <p>question: Is this patient in a supine position?</p>	<p>Text-Prompt:</p> <p>Input an X-ray image along with a question..... (VQA Prompt)</p> <p>=====</p> <p>question: Is the lesion a solid or cystic lesion?</p>
	
<p>Ground Truth:</p> <p>Yes</p>	<p>Ground Truth:</p> <p>No</p>
<p>GPT-4V:</p> <p>Closed-ended Question answer: Yes.</p>	<p>GPT-4V:</p> <p>Closed-ended Question answer: No.</p>

Fig. 13. VQA case examples for close-end questions. By few-shot prompts, GPT-4V could discern the question type and generate correct “yes” or “no” answers.

Visual Grounding Cases

In Figure 15 we provide two examples that shed light on GPT-4V’s performance in visual grounding tasks. Our examination suggests that while GPT-4V exhibits the capability to generate bounding boxes, its performance is suboptimal, especially in precisely locating objects within images. This limitation might stem from GPT-4V’s challenges in processing and interpreting detailed image information, particularly in the context of medical images where a nuanced focus on fine-grid features is crucial for accurate visual grounding. Furthermore, we posit that GPT-4V’s training, predominantly on common images, may contribute to its suboptimal performance with medical images. The model’s limited exposure to diverse and labelled medical data might be a key factor in this inadequacy.

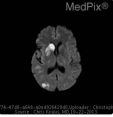
Visual Question Answering Cases (Close-end Questions)	
<p>Text-Prompt: Input an X-ray image along with a question..... (VQA Prompt) =====</p> <p>question: What organ system is shown in the above image?</p>  <p>Ground Truth: Brain</p> <p>GPT-4V: Open-ended Question answer: Brain.</p>	<p>Text-Prompt: Input an X-ray image along with a question..... (VQA Prompt) =====</p> <p>question: What brain structures would be affected by the lesion in the right frontal area of the brain?</p>  <p>Ground Truth: basal ganglia (caudate and putamen)</p> <p>GPT-4V: Open-ended Question answer: The lesion in the right frontal area of the brain would affect the right frontal lobe structures including the prefrontal cortex, primary motor cortex, and possibly the premotor and precentral gyrus.</p>

Fig. 14. VQA case examples for open-end questions. By few-shot prompts, GPT-4V has the capacity to generate correct answers (left). However, it may sometimes overlook visual information and generate answers solely based on general medical knowledge (right).

Visual Grounding Cases	
<p>Text-Prompt: You are a radiological AI assistant.....(VG Prompt) =====</p> <p>Image Dimensions: {width: 1767, height: 2021} The descriptive text is: Large right-sided pneumothora</p> <p>GPT-4V: [top left x: 400, top left y: 100, width: 350, height: 600]</p> <p>Ground Truth: [265, 90, 880, 2198]</p>	<p>Image Prompt:</p>  <p>Bounding Box:</p> 
<p>Text-Prompt: You are a radiological AI assistant.....(VG Prompt) =====</p> <p>Image Dimensions: {width: 2539, height: 3050} The descriptive text is: Bilateral multifocal areas of consolidation</p> <p>GPT-4V: [top left x: 130, top left y: 350, width: 650, height: 300]</p> <p>Ground Truth: [1510, 1268, 755, 796]</p>	<p>Image Prompt:</p>  <p>Bounding Box:</p> 

Fig. 15. Visual Grounding Prompt case. The bounding boxes in red are predicted by GPT-4V, while the ground truth bounding boxes are in green.

4. Summary and discussion

This study thoroughly investigates GPT-4V’s performance in three key medical applications, employing a comprehensive evaluation methodology encompassing quantitative analysis, human assessment, and case studies.

In the domain of radiology report generation, GPT-4V effectively generates radiology reports from medical images, close to models specially trained for this task in language fluency and clinical relevance. Human evaluations reveal its higher accuracy and detailed generation, suggesting conventional metrics fall short in assessing LLMs like GPT-4V. Beyond quantitative analysis, notable observations include the impact of different prompts on GPT-4V’s report generation. Specifically, a mixed-example prompt, incorporating both normal and abnormal cases, enhances report quality compared to prompts with solely normal or abnormal examples. Also, it is found that GPT-4V’s ability to generate additional information not

present in the ground truth, though visible in images, contributes to relatively lower BLEU scores that focus on word-matching rates, compared to specially trained R2Gen models. Remarkably, GPT-4V exhibits a notably lower CIDEr score than conventional R2Gen models, consistent with findings from R2GenGPT (Wang et al., 2023b), which employed a frozen LLM for medical report generation. This lower CIDEr score may suggest a tendency of LLMs to generate repetitive description patterns. Meanwhile, when evaluating the rank correlation between NLP/clinical scores and the human rating, the latter aligns more closely with clinical scores than NLP scores, consistent with the observation that GPT-4V exhibits competitive clinical efficacy close to high-performing R2Gen models.

In the domain of medical visual question answering, GPT-4V exhibits promise but achieves modest scores when compared to advanced methods, primarily due to the low correlation of its answers with standard benchmarks. It is noteworthy that human assessments consistently rate its accuracy higher than these metrics suggest. Meanwhile, several limitations associated with the VQA datasets and evaluation call for attention. The current public datasets for VQA are constrained by a fixed answer format, imposing limitations on the training potential of models like GPT-4V and introducing challenges in accurately evaluating their performance. The inherent rigidity of these datasets becomes apparent when assessing generative models for VQA, where a more flexible evaluation approach to accommodate a spectrum of correct answers is warranted. Moreover, the predominant method for evaluating VQA tasks, rooted in classification techniques, centers around accuracy. This approach becomes less effective when transitioning to large models like LLMs for VQA tasks. Compared with traditional methods, LLMs generate answers in a more flexible and nuanced manner, leading to a variety of correct answers that may not align with the limited set of predefined ground truth and thus could be unfairly marked as incorrect by conventional evaluation metrics. Consequently, there is a pressing need for more sophisticated evaluation methods, which should be adept at assessing contextual and semantic correctness, departing from the conventional practice of exact matches with predefined correct answers. Such an evolved approach would provide a more accurate gauge of LLMs’ capabilities in comprehending and responding to the intricacies of VQA tasks, thereby reflecting the true potential of these advanced models in handling complex question-answering scenarios.

In the domain of medical visual grounding, GPT-4V exhibits a need for refinement in accurately locating and identifying specific image elements, echoing a recognized gap observed in generic image tasks. This underscores a notable area for potential improvement. A recent publication Yang et al. (2023a) introduced the Set-of-Mark prompting method, offering a novel approach to enhance the visual grounding capabilities of large multimodal models, including GPT-4V. The SoM method entails partitioning an image into regions and overlaying them with marks, such as alphanumeric characters, masks, or boxes. These marks serve to augment GPT-4V’s understanding and responsiveness to visual content, leading to a significant enhancement in performance, particularly in fine-grained vision

tasks within a zero-shot setting. This innovative method holds promise for addressing the identified need for improvement in GPT-4V’s performance in medical image visual grounding. In the medical context, where precise identification and description of specific regions or features in images are crucial, applying the SoM technique could potentially empower models like GPT-4V to provide more accurate and detailed descriptions of medical images, thereby contributing to improved diagnosis and treatment planning.

Overall, our evaluation, incorporating standard metrics and medical expert reviews, underscores the limitations of traditional methods in fully capturing GPT-4V’s capabilities, emphasizing the imperative for improved evaluation techniques tailored to large language models.

5. Conclusion and limitation

Our comprehensive evaluation of GPT-4V across key medical applications sheds light on its remarkable capabilities and areas for refinement. GPT-4V substantially enhances text generation capabilities in multi-modal contexts. Its proficiency in generating nuanced and contextually relevant text underscores its potential to revolutionize medical applications that demand a profound understanding of both text and imagery.

While our study provides valuable insights, certain limitations present opportunities for enhancement in future research. First, our human evaluation, based on 100 cases, aligns with similar studies in the literature; however, the sample size remains relatively small, offering a representative but limited perspective on the issues discussed. Second, our human evaluation employs a grading system with three basic levels. This categorization, while providing a general understanding, is somewhat rudimentary. Future studies could benefit from a more detailed and nuanced human evaluation framework, potentially offering more granular insights into model performance and efficiency in the assessment process. Further refinement in evaluation methodologies would contribute to a more comprehensive understanding of the intricacies involved in model assessments.

References

- Ambati, R., Dudyala, C.R., 2018. A sequence-to-sequence model approach for imageclef 2018 medical domain visual question answering, in: 2018 15th IEEE India Council International Conference (INDICON), IEEE. pp. 1–6.
- Anil, R., Dai, A.M., Firat, O., Johnson, M., Lepikhin, D., Passos, A., Shakeri, S., Taropa, E., Bailey, P., Chen, Z., et al., 2023. Palm 2 technical report. arXiv preprint arXiv:2305.10403 .
- Awadalla, A., Gao, I., Gardner, J., Hessel, J., Hanafy, Y., Zhu, W., Marathe, K., Bitton, Y., Gadre, S., Sagawa, S., et al., 2023. Openflamingo: An open-source framework for training large autoregressive vision-language models. arXiv preprint arXiv:2308.01390 .
- Banerjee, S., Lavie, A., 2005. METEOR: an automatic metric for MT evaluation with improved correlation with human judgments, in: Goldstein, J., Lavie, A., Lin, C., Voss, C.R. (Eds.), Proceedings of the Workshop on Intrinsic and Extrinsic Evaluation Measures for Machine Translation and/or Summarization@ACL 2005, Ann Arbor, Michigan, USA, June 29, 2005, Association for Computational Linguistics. pp. 65–72. URL: <https://aclanthology.org/w05-0909/>.
- Bannur, S., Hyland, S., Liu, Q., Perez-Garcia, F., Ilse, M., Castro, D.C., Boecking, B., Sharma, H., Bouzid, K., Thieme, A., et al., 2023. Learning to exploit temporal structure for biomedical vision-language processing, in: Proceedings of the IEEE/CVF Conference on Computer Vision and Pattern Recognition, pp. 15016–15027.
- Boecking, B., Usuyama, N., Bannur, S., Castro, D.C., Schwaighofer, A., Hyland, S., Wetscherek, M., Naumann, T., Nori, A., Alvarez-Valle, J., et al., 2022. Making the most of text semantics to improve biomedical vision-language processing, in: European conference on computer vision, Springer. pp. 1–21.
- Chen, Z., Shen, Y., Song, Y., Wan, X., 2021. Cross-modal memory networks for radiology report generation, in: Zong, C., Xia, F., Li, W., Navigli, R. (Eds.), Proceedings of the 59th Annual Meeting of the Association for Computational Linguistics and the 11th International Joint Conference on Natural Language Processing, ACL/IJCNLP 2021, (Volume 1: Long Papers), Virtual Event, August 1-6, 2021, Association for Computational Linguistics. pp. 5904–5914. URL: <https://doi.org/10.18653/v1/2021.acl-long.459>, doi:10.18653/v1/2021.acl-long.459.
- Chen, Z., Song, Y., Chang, T., Wan, X., 2020. Generating radiology reports via memory-driven transformer, in: Webber, B., Cohn, T., He, Y., Liu, Y. (Eds.), Proceedings of the 2020 Conference on Empirical Methods in Natural Language Processing, EMNLP 2020, Online, November 16-20, 2020, Association for Computational Linguistics. pp. 1439–1449. URL: <https://doi.org/10.18653/v1/2020.emnlp-main.112>, doi:10.18653/v1/2020.emnlp-main.112.
- Chen, Z., Zhou, Y., Tran, A., Zhao, J., Wan, L., Ooi, G.S.K., Cheng, L.T.E., Thng, C.H., Xu, X., Liu, Y., et al., 2023. Medical phrase grounding with region-phrase context contrastive alignment, in: International Conference on Medical Image Computing and Computer-Assisted Intervention, Springer. pp. 371–381.
- Cornia, M., Stefanini, M., Baraldi, L., Cucchiara, R., 2020. Meshed-memory transformer for image captioning, in: 2020 IEEE/CVF Conference on Computer Vision and Pattern Recognition, CVPR 2020, Seattle, WA, USA, June 13-19, 2020, Computer Vision Foundation / IEEE. pp. 10575–10584. URL: https://openaccess.thecvf.com/content_CVPR_2020/html/Cornia_Meshed-Memory_Transformer_for_Image_Captioning_CVPR_2020_paper.html, doi:10.1109/CVPR42600.2020.01059.
- Dai, D., Sun, Y., Dong, L., Hao, Y., Sui, Z., Wei, F., 2022. Why can gpt learn in-context? language models secretly perform gradient descent as meta optimizers. arXiv preprint arXiv:2212.10559 .
- Deng, J., Yang, Z., Chen, T., Zhou, W., Li, H., 2021. Transvg: End-to-end visual grounding with transformers, in: Proceedings of the IEEE/CVF International Conference on Computer Vision, pp. 1769–1779.
- Do, T., Nguyen, B.X., Tjiputra, E., Tran, M., Tran, Q.D., Nguyen, A., 2021. Multiple meta-model quantifying for medical visual question answering, in: International Conference on Medical Image Computing and Computer-Assisted Intervention, Springer. pp. 64–74.
- Du, Y., Fu, Z., Liu, Q., Wang, Y., 2022. Visual grounding with transformers, in: 2022 IEEE International Conference on Multimedia and Expo (ICME), IEEE. pp. 1–6.
- Eslami, S., de Melo, G., Meinel, C., 2021. Does clip benefit visual question answering in the medical domain as much as it does in the general domain? arXiv preprint arXiv:2112.13906 .
- Finn, C., Abbeel, P., Levine, S., 2017. Model-agnostic meta-learning for fast adaptation of deep networks, in: International conference on machine learning, PMLR. pp. 1126–1135.
- He, X., Zhang, Y., Mou, L., Xing, E., Xie, P., 2020. Pathvqa: 30000+ questions for medical visual question answering. arXiv preprint arXiv:2003.10286 .
- Huang, W., Zhou, H., Li, C., Yang, H., Liu, J., Wang, S., 2023a. Enhancing representation in radiography-reports foundation model: A granular alignment algorithm using masked contrastive learning. arXiv preprint arXiv:2309.05904 .
- Huang, Z., Zhang, X., Zhang, S., 2023b. Kiut: Knowledge-injected u-transformer for radiology report generation, in: Proceedings of the IEEE/CVF Conference on Computer Vision and Pattern Recognition, pp. 19809–19818.
- Jiang, H., Misra, I., Rohrbach, M., Learned-Miller, E., Chen, X., 2020. In defense of grid features for visual question answering, in: Proceedings of the IEEE/CVF Conference on Computer Vision and Pattern Recognition, pp. 10267–10276.
- Johnson, A.E.W., Pollard, T.J., Berkowitz, S.J., Greenbaum, N.R., Lungren, M.P., Deng, C., Mark, R.G., Horng, S., 2019. MIMIC-CXR: A large publicly available database of labeled chest radiographs. CoRR abs/1901.07042. URL: <http://arxiv.org/abs/1901.07042>, arXiv:1901.07042.

- Kamath, A., Singh, M., LeCun, Y., Synnaeve, G., Misra, I., Carion, N., 2021. Mdetr-modulated detection for end-to-end multi-modal understanding, in: Proceedings of the IEEE/CVF International Conference on Computer Vision, pp. 1780–1790.
- Khare, Y., Bagal, V., Mathew, M., Devi, A., Priyakumar, U.D., Jawahar, C., 2021. Mmbert: multimodal bert pretraining for improved medical vqa, in: 2021 IEEE 18th International Symposium on Biomedical Imaging (ISBI), IEEE, pp. 1033–1036.
- Lau, J.J., Gayen, S., Ben Abacha, A., Demner-Fushman, D., 2018. A dataset of clinically generated visual questions and answers about radiology images. *Scientific data* 5, 1–10.
- Li, C., Wong, C., Zhang, S., Usuyama, N., Liu, H., Yang, J., Naumann, T., Poon, H., Gao, J., 2023a. Llava-med: Training a large language-and-vision assistant for biomedicine in one day. *arXiv preprint arXiv:2306.00890*.
- Li, J., Li, D., Savarese, S., Hoi, S., 2023b. Blip-2: Bootstrapping language-image pre-training with frozen image encoders and large language models. *arXiv preprint arXiv:2301.12597*.
- Li, M., Lin, B., Chen, Z., Lin, H., Liang, X., Chang, X., 2023c. Dynamic graph enhanced contrastive learning for chest x-ray report generation, in: Proceedings of the IEEE/CVF Conference on Computer Vision and Pattern Recognition, pp. 3334–3343.
- Li, M., Sigal, L., 2021. Referring transformer: A one-step approach to multi-task visual grounding. *Advances in neural information processing systems* 34, 19652–19664.
- Li, Y., Liang, X., Hu, Z., Xing, E.P., 2018. Hybrid retrieval-generation reinforced agent for medical image report generation, in: Bengio, S., Wallach, H.M., Larochelle, H., Grauman, K., Cesa-Bianchi, N., Garnett, R. (Eds.), *Advances in Neural Information Processing Systems 31: Annual Conference on Neural Information Processing Systems 2018, NeurIPS 2018, December 3-8, 2018, Montréal, Canada*, pp. 1537–1547. URL: <https://proceedings.neurips.cc/paper/2018/hash/e07413354875be01a996dc560274708e-Abstract.html>.
- Li, Y., Wang, L., Hu, B., Chen, X., Zhong, W., Lyu, C., Zhang, M., 2023d. A comprehensive evaluation of gpt-4v on knowledge-intensive visual question answering. *arXiv preprint arXiv:2311.07536*.
- Lin, C.Y., 2004. ROUGE: A package for automatic evaluation of summaries, in: *Text Summarization Branches Out*, Association for Computational Linguistics, Barcelona, Spain, pp. 74–81. URL: <https://aclanthology.org/W04-1013>.
- Liu, F., Wu, X., Ge, S., Fan, W., Zou, Y., 2021a. Exploring and distilling posterior and prior knowledge for radiology report generation, in: Proceedings of the IEEE/CVF conference on computer vision and pattern recognition, pp. 13753–13762.
- Liu, F., Wu, X., Ge, S., Fan, W., Zou, Y., 2021b. Exploring and distilling posterior and prior knowledge for radiology report generation, in: *IEEE Conference on Computer Vision and Pattern Recognition, CVPR 2021, virtual, June 19-25, 2021, Computer Vision Foundation / IEEE*, pp. 13753–13762. URL: https://openaccess.thecvf.com/content/CVPR2021/html/Liu_Exploring_and_Distilling_Posterior_and_Prior_Knowledge_for_Radiology_Report_CVPR_2021_paper.html, doi:10.1109/CVPR46437.2021.01354.
- Liu, Y., Wang, Z., Xu, D., Zhou, L., 2023. Q2atransformer: Improving medical vqa via an answer querying decoder, in: *International Conference on Information Processing in Medical Imaging*, Springer, pp. 445–456.
- Lu, J., Xiong, C., Parikh, D., Socher, R., 2017. Knowing when to look: Adaptive attention via a visual sentinel for image captioning, in: *2017 IEEE Conference on Computer Vision and Pattern Recognition, CVPR 2017, Honolulu, HI, USA, July 21-26, 2017, IEEE Computer Society*, pp. 3242–3250. URL: <https://doi.org/10.1109/CVPR.2017.345>, doi:10.1109/CVPR.2017.345.
- Nguyen, B.D., Do, T.T., Nguyen, B.X., Do, T., Tjiputra, E., Tran, Q.D., 2019. Overcoming data limitation in medical visual question answering, in: *International Conference on Medical Image Computing and Computer-Assisted Intervention*, Springer, pp. 522–530.
- OpenAI, 2023. Gpt-4 technical report. *ArXiv abs/2303.08774*. URL: <https://api.semanticscholar.org/CorpusID:257532815>.
- Pan, Y., Yao, T., Li, Y., Mei, T., 2020. X-linear attention networks for image captioning, in: *2020 IEEE/CVF Conference on Computer Vision and Pattern Recognition, CVPR 2020, Seattle, WA, USA, June 13-19, 2020, Computer Vision Foundation / IEEE*, pp. 10968–10977. URL: https://openaccess.thecvf.com/content_CVPR_2020/html/Pan_X-Linear_Attention_Networks_for_Image_Captioning_CVPR_2020_paper.html, doi:10.1109/CVPR42600.2020.01098.
- Papineni, K., Roukos, S., Ward, T., Zhu, W., 2002. Bleu: a method for automatic evaluation of machine translation, in: *Proceedings of the 40th Annual Meeting of the Association for Computational Linguistics, July 6-12, 2002, Philadelphia, PA, USA, ACL*, pp. 311–318. URL: <https://aclanthology.org/P02-1040/>, doi:10.3115/1073083.1073135.
- Pellegrini, C., Keicher, M., Özsoy, E., Navab, N., 2023. Rad-restruct: A novel vqa benchmark and method for structured radiology reporting, in: *International Conference on Medical Image Computing and Computer-Assisted Intervention*, Springer, pp. 409–419.
- Peng, Z., Wang, W., Dong, L., Hao, Y., Huang, S., Ma, S., Wei, F., 2023. Kosmos-2: Grounding multimodal large language models to the world. *arXiv preprint arXiv:2306.14824*.
- Shi, Y., Peng, D., Liao, W., Lin, Z., Chen, X., Liu, C., Zhang, Y., Jin, L., 2023. Exploring ocr capabilities of gpt-4v (ision): A quantitative and in-depth evaluation. *arXiv preprint arXiv:2310.16809*.
- Singhal, K., Tu, T., Gottweis, J., Sayres, R., Wulczyn, E., Hou, L., Clark, K., Pfohl, S., Cole-Lewis, H., Neal, D., et al., 2023. Towards expert-level medical question answering with large language models. *arXiv preprint arXiv:2305.09617*.
- Sun, J., Wei, D., Xu, Z., Lu, D., Liu, H., Wang, L., Zheng, Y., 2023a. You’ve got two teachers: Co-evolutionary image and report distillation for semi-supervised anatomical abnormality detection in chest x-ray, in: *International Conference on Medical Image Computing and Computer-Assisted Intervention*, Springer, pp. 363–373.
- Sun, Z., Lin, M., Zhu, Q., Xie, Q., Wang, F., Lu, Z., Peng, Y., 2023b. A scoping review on multimodal deep learning in biomedical images and texts. *Journal of Biomedical Informatics*, 104482.
- Touvron, H., Lavril, T., Izacard, G., Martinet, X., Lachaux, M.A., Lacroix, T., Rozière, B., Goyal, N., Hambro, E., Azhar, F., et al., 2023. Llama: Open and efficient foundation language models. *arXiv preprint arXiv:2302.13971*.
- Tsimpoukelli, M., Menick, J.L., Cabi, S., Eslami, S., Vinyals, O., Hill, F., 2021. Multimodal few-shot learning with frozen language models. *Advances in Neural Information Processing Systems* 34, 200–212.
- Vaswani, A., Shazeer, N., Parmar, N., Uszkoreit, J., Jones, L., Gomez, A.N., Kaiser, L., Polosukhin, I., 2017. Attention is all you need, in: *Guyon, I., von Luxburg, U., Bengio, S., Wallach, H.M., Fergus, R., Vishwanathan, S.V.N., Garnett, R. (Eds.), Advances in Neural Information Processing Systems 30: Annual Conference on Neural Information Processing Systems 2017, December 4-9, 2017, Long Beach, CA, USA*, pp. 5998–6008. URL: <https://proceedings.neurips.cc/paper/2017/hash/3f5ee243547dee91fbd053c1c4a845aa-Abstract.html>.
- Vedantam, R., Zitnick, C.L., Parikh, D., 2015. Cider: Consensus-based image description evaluation, in: *IEEE Conference on Computer Vision and Pattern Recognition, CVPR 2015, Boston, MA, USA, June 7-12, 2015, IEEE Computer Society*, pp. 4566–4575. URL: <https://doi.org/10.1109/CVPR.2015.7299087>, doi:10.1109/CVPR.2015.7299087.
- Vinyals, O., Toshev, A., Bengio, S., Erhan, D., 2015. Show and tell: A neural image caption generator, in: *IEEE Conference on Computer Vision and Pattern Recognition, CVPR 2015, Boston, MA, USA, June 7-12, 2015, IEEE Computer Society*, pp. 3156–3164. URL: <https://doi.org/10.1109/CVPR.2015.7298935>, doi:10.1109/CVPR.2015.7298935.
- Wang, X., Wei, J., Schuurmans, D., Le, Q., Chi, E., Narang, S., Chowdhery, A., Zhou, D., 2022a. Self-consistency improves chain of thought reasoning in language models. *arXiv preprint arXiv:2203.11171*.
- Wang, Z., Liu, L., Wang, L., Zhou, L., 2023a. Metransformer: Radiology report generation by transformer with multiple learnable expert tokens, in: *IEEE/CVF Conference on Computer Vision and Pattern Recognition, CVPR 2023, Vancouver, BC, Canada, June 17-24, 2023, IEEE*, pp. 11558–11567. URL: <https://doi.org/10.1109/CVPR52729.2023.01112>, doi:10.1109/CVPR52729.2023.01112.
- Wang, Z., Liu, L., Wang, L., Zhou, L., 2023b. R2genpt: Radiology report generation with frozen llms. *arXiv preprint arXiv:2309.09812*.
- Wang, Z., Tang, M., Wang, L., Li, X., Zhou, L., 2022b. A medical semantic-assisted transformer for radiographic report generation, in: *Wang, L., Dou, Q., Fletcher, P.T., Speidel, S., Li, S. (Eds.), Medical Image Computing and Computer Assisted Intervention - MICCAI 2022 - 25th International Conference, Singapore, September 18-22, 2022, Proceedings, Part III, Springer*, pp. 655–664. URL: https://doi.org/10.1007/978-3-031-16437-8_63, doi:10.1007/978-3-031-16437-8_63.
- Wei, J., Tay, Y., Bommasani, R., Raffel, C., Zoph, B., Borgeaud, S., Yogatama,

- D., Bosma, M., Zhou, D., Metzler, D., et al., 2022a. Emergent abilities of large language models. arXiv preprint arXiv:2206.07682 .
- Wei, J., Wang, X., Schuurmans, D., Bosma, M., Xia, F., Chi, E., Le, Q.V., Zhou, D., et al., 2022b. Chain-of-thought prompting elicits reasoning in large language models. *Advances in Neural Information Processing Systems* 35, 24824–24837.
- Wu, C., Lei, J., Zheng, Q., Zhao, W., Lin, W., Zhang, X., Zhou, X., Zhao, Z., Zhang, Y., Wang, Y., et al., 2023a. Can gpt-4v (ision) serve medical applications? case studies on gpt-4v for multimodal medical diagnosis. arXiv preprint arXiv:2310.09909 .
- Wu, C., Liu, J., Wang, X., Li, R., 2019. Differential networks for visual question answering, in: *Proceedings of the AAAI Conference on Artificial Intelligence*, pp. 8997–9004.
- Wu, Y., Wang, S., Yang, H., Zheng, T., Zhang, H., Zhao, Y., Qin, B., 2023b. An early evaluation of gpt-4v (ision). arXiv preprint arXiv:2310.16534 .
- Xu, K., Ba, J., Kiros, R., Cho, K., Courville, A.C., Salakhutdinov, R., Zemel, R.S., Bengio, Y., 2015. Show, attend and tell: Neural image caption generation with visual attention, in: *Bach, F.R., Blei, D.M. (Eds.), Proceedings of the 32nd International Conference on Machine Learning, ICML 2015, Lille, France, 6-11 July 2015, JMLR.org*, pp. 2048–2057. URL: <http://proceedings.mlr.press/v37/xuc15.html>.
- Yang, J., Zhang, H., Li, F., Zou, X., Li, C., Gao, J., 2023a. Set-of-mark prompting unleashes extraordinary visual grounding in gpt-4v. arXiv preprint arXiv:2310.11441 .
- Yang, S., Wu, X., Ge, S., Zhou, S.K., Xiao, L., 2021. Knowledge matters: Radiology report generation with general and specific knowledge. *Medical Image Analysis* .
- Yang, Z., Li, L., Lin, K., Wang, J., Lin, C.C., Liu, Z., Wang, L., 2023b. The dawn of llms: Preliminary explorations with gpt-4v (ision). arXiv preprint arXiv:2309.17421 .
- Ye, Q., Xu, H., Xu, G., Ye, J., Yan, M., Zhou, Y., Wang, J., Hu, A., Shi, P., Shi, Y., et al., 2023. mplug-owl: Modularization empowers large language models with multimodality. arXiv preprint arXiv:2304.14178 .
- Zhang, Y., Wang, X., Xu, Z., Yu, Q., Yuille, A., Xu, D., 2020. When radiology report generation meets knowledge graph. *Proceedings of the AAAI Conference on Artificial Intelligence* .
- Zhao, Y., Lin, Z., Zhou, D., Huang, Z., Feng, J., Kang, B., 2023. Bubogpt: Enabling visual grounding in multi-modal llms. arXiv preprint arXiv:2307.08581 .
- Zhu, C., Zhou, Y., Shen, Y., Luo, G., Pan, X., Lin, M., Chen, C., Cao, L., Sun, X., Ji, R., 2022. Seqtr: A simple yet universal network for visual grounding, in: *European Conference on Computer Vision, Springer*, pp. 598–615.

Appendix A. Appendix

Appendix A.1. Details of Prompt Settings

To elucidate our prompt design and selection process, we present illustrative cases for better comprehension. We show-case instances involving both zero-shot and few-shot prompts to elucidate the distinction. In the zero-shot scenario, the model relies solely on its inherent training and knowledge base. Conversely, the few-shot scenario incorporates specific examples, enhancing the model’s understanding and response accuracy. Our few-shot prompt encompasses diverse cases utilising both normal and abnormal examples, showcasing radiology images with normal and abnormal findings. In all prompts, we prompt GPT-4V to assume the role of a professional radiologist. Additionally, we explicitly instruct it to generate both the impression and findings sections.

Appendix A.1.1. Zero-shot prompt

Figure A.16 showcases a zero-shot prompt example. We did not add any additional information to the text prompt.

Zero-shot Prompt

<p>Text-Prompt:</p> <p>You are a professional radiologist. I will provide you with some chest X-ray images. Please generate a radiology report based on the provided image. The report needs to contain both the impression and findings sections. You should only generate reports and no other unnecessary information.</p>	<p>Image:</p> 
<p>GPT-4V:</p> <p>Impression: Normal chest radiograph with no acute cardiopulmonary abnormalities. Findings: Lungs: Clear bilaterally. No focal opacity, consolidation, or mass identified. Cardiomediastinal silhouette: Normal size and contour. No mediastinal widening. Bones: Intact without any appreciable fractures or bony lesions. Diaphragm: Intact with no evidence of diaphragmatic hernia. Soft tissues: Unremarkable.</p>	
<p>Ground Truth:</p> <p>impression: No acute intrathoracic process. Findings: The lungs are well expanded and clear. The cardiomeastinal silhouette, hilar contours, and pleural surfaces are normal. No pleural effusion or pneumothorax is present. Sternal wires are intact.</p>	

Fig. A.16. Zero-shot prompt. No additional information provided to GPT-4V.

Appendix A.1.2. Few-shot prompt

We add two example reports to the prompt while exploring three different combinations: (1) exclusively using normal examples, (2) exclusively using abnormal examples), (3) combining one normal and one abnormal example. The example reports are given in Figure A.17.

Few-shot normal examples prompt In this prompt method, we curated reports from two normal samples within the MIMIC-CXR training set. To ensure comprehensiveness, we specifically chose reports with rich content.

Few-shot abnormal examples prompt In this prompt method, we carefully chose two reports originating from abnormal samples within the MIMIC-CXR training set.

Few-shot abnormal examples prompt
<p>Case 1: Impression: Mediastinal widening more than expected given procedure, concerning for substantial mediastinal hemorrhage. Left chest tube in place with no pneumothorax. Findings: Mediastinum is widened and is more than expected status post bisegmentectomy concerning for substantial mediastinal hemorrhage with indentation of the left tracheal wall contour. Patient is status post left upper lobe bisegmentectomy with left chest tube in place. Bilateral low lung volumes. No pneumothorax. Pleural effusions little if any. Cardiac size appears enlarged and likely is exaggerated by low lung volumes.</p> <p>Case 2: Impression: Focal consolidation at the left lung base, possibly representing aspiration or pneumonia. Central vascular engorgement. Findings: PA and lateral views of the chest provided. The lungs are adequately aerated. There is a focal consolidation at the left lung base adjacent to the lateral hemidiaphragm. There is mild vascular engorgement. There is bilateral apical pleural thickening. The cardiomediastinal silhouette is remarkable for aortic arch calcifications. The heart is top normal in size.</p>
Few-shot normal examples prompt
<p>Case 1: Impression: No acute cardiopulmonary process. Findings: There is no focal consolidation. Pleural effusion or pneumothorax. Bilateral nodular opacities that most likely represent nipple shadows. The cardiomediastinal silhouette is normal. Clips project over the left lung, potentially within the breast. The imaged upper abdomen is unremarkable.</p> <p>Case 2: Impression: No evidence of pneumonia. Findings: The lung volumes are normal. Normal hilar and mediastinal structures. No pneumonia, no pulmonary edema. No pleural effusions. Status post CABG with aligned median sternotomy wires and normal location of surgical clips. Status post right lung surgery with surgical material seen.</p>
Few-shot mixed examples prompt
<p>Case 1: Impression: Retrocardiac opacity, potentially atelectasis, though infection cannot be excluded in the correct clinical setting. Persistent elevation of the right hemidiaphragm with right basilar atelectasis. Findings: Mild cardiomegaly with a left ventricular predominance is re-demonstrated. The mediastinal and hilar contours are unchanged. Pulmonary vasculature is normal. Elevation of the right hemidiaphragm is again noted with associated right basilar atelectasis. Retrocardiac patchy opacity may reflect atelectasis though infection is not excluded in the correct clinical setting. No pleural effusion or pneumothorax is detected. S-shaped rotary scoliosis of the thoracolumbar spine is again noted.</p> <p>Case 2: Impression: No evidence of pneumonia. Findings: Frontal and lateral views of the chest demonstrate no focal consolidation. Except for linear atelectasis in the right lower lung, the lungs are clear. The cardiomediastinal and hilar contours are normal. There is no pneumothorax or pleural effusion. Pleural surfaces are normal.</p>

Fig. A.17. Example reports in prompts: Three pairs of different example reports in few-shot prompt settings. We added these example reports to few-shot prompts to help GPT-4V generate radiology reports.

Few-shot mixed-example prompt In this prompt method, we chose one normal and one abnormal report from the MIMIC-CXR training set. The sequence in which these two examples are presented is not anticipated to significantly impact the generated results. In this specific experiment, we positioned the abnormal report before the normal one.